

# SI: Two-Dimensional Multifunctional Metal–Organic Framework with large In-Plane Negative Poisson Ratio and Photocatalytic Water Splitting Properties

Wei Lin,<sup>†</sup> Huimiao Wang,<sup>‡</sup> Yaling Luo,<sup>¶</sup> Xiaofeng Liu,<sup>†</sup> Zhongjun Li,<sup>†</sup> Weiduo  
Zhu,<sup>†</sup> Xingxing Li,<sup>§</sup> Zhao Chen,<sup>\*,†</sup> and Haidi Wang<sup>\*,†</sup>

<sup>†</sup>*School of Physics, Hefei University of Technology, Hefei, Anhui 230009, China*

<sup>‡</sup>*School of Civil and Hydraulic Engineering, Hefei University of Technology, Xuancheng,  
Anhui 230002, China*

<sup>¶</sup>*School of Materials Science and Engineering, Hefei University of Technology, Xuancheng,  
Anhui 230002, China*

<sup>§</sup> *Hefei National Laboratory for Physical Sciences at Microscale, Department of Chemical  
Physics, and Synergetic Innovation Center of Quantum Information and Quantum Physics,  
University of Science and Technology of China, Hefei, Anhui 230026, China*

E-mail: chenzhao@hfut.edu.cn; haidi@hfut.edu.cn

## Computational Methods

First-principles density functional theory (DFT) calculations are conducted by the Vienna ab initio simulation package (VASP) software package.<sup>1</sup> The generalized gradient approximation (GGA) of Perdew, Burke, and Ernzerhof (PBE) exchange correlation functional<sup>2</sup> and plane

wave basis set are used to describe the valence electrons with the cutoff set to 520 eV.<sup>3</sup> The energy convergence criteria for electronic wavefunction was set to be  $1.0 \times 10^{-5}$  eV. The geometry optimization was converged when the force on each atom was smaller than  $0.5 \times 10^{-3}$  eV·Å<sup>-1</sup>. The  $8 \times 8 \times 1$  Monkhorst-Pack k-point mesh was used to sample the Brillouin zone.<sup>4</sup>

Hybrid functional (HSE06) calculations with 25% Hartree-Fock exchange are used to calculate more reliable band structures.<sup>5,6</sup> The thermostability of M<sub>2</sub>C<sub>4</sub>X<sub>4</sub> is checked by conducting *ab initio* molecular dynamics (AIMD) simulations for 10 ps with a time step of 1.0 fs at 300 K controlled by a Nosé-Hoover thermostat. The Phonopy code interfaced with the VASP is used to calculate the phonon spectrum. The DFT-D3 method with Becke-Jonson damping is used to account for the effect of the vdW interaction between absorbates with substrate.

The basic mechanical properties, such as elastic constants, Young's modulus, shear modulus and Poisson's ratio are calculate by our mech2d<sup>1</sup> package with VASP interface. For a 2D material with square lattice, the independent elastic constant are  $C_{11}$ ,  $C_{12}$  and  $C_{66}$ . The corresponding strain energy-strain equation can be written as:<sup>7</sup>

$$E(\boldsymbol{\eta}) = E_0 + \frac{AC_{11}\eta_1^2}{2} + \frac{AC_{11}\eta_2^2}{2} + AC_{12}\eta_1\eta_2 + \frac{AC_{66}\eta_6^2}{2} \quad (1)$$

where,  $A$  is area of the 2D system and the Lagrangian strain tensor  $\boldsymbol{\eta}$  is represented as a vector:  $\boldsymbol{\eta} = (\eta_1, \eta_2, 0, 0, 0, \eta_6)$ . To simplify the above equation, a set of deformation need to be applied. In this work, the selected deformation set are bi-axial strain ( $\boldsymbol{\eta} = (\eta, \eta, 0, 0, 0, 0)$ ), uni-axial strain ( $\boldsymbol{\eta} = (\eta, 0, 0, 0, 0, 0)$ ) and shear strain ( $\boldsymbol{\eta} = (0, 0, 0, 0, 0, 2\eta)$ ). The max strain amplitude is set to 0.02. Finally, via fitting the above strain energy-strain equation, the elastic constant can be calculated.

To investigate the strain response, the deformation of a structure under external stresses applied at arbitrary angles  $\theta$  can be determined by the following formula:

---

<sup>1</sup>mech2d <https://github.com/haidi-ustc/mech2d>

$$\nu(\theta) = \frac{C_{11} \cos^4 \theta - \left( C_{11} + C_{22} - \frac{C_{11}C_{22}-C_{12}^2}{C_{66}} \right) \cos^2 \theta \sin^2 \theta + C_{12} \sin^4 \theta}{C_{22} \cos^4 \theta - \left( 2C_{12} - \frac{C_{11}C_{22}-C_{12}^2}{C_{66}} \right) \cos^2 \theta \sin^2 \theta + C_{11} \sin^4 \theta} \quad (2)$$

$$\epsilon(\theta) = \sigma \left( \frac{C_{11}C_{22} \cos^4 \theta - 2C_{12} \cos^2 \theta \sin^2 \theta + C_{11} \sin^4 \theta}{C_{11}C_{22} - C_{12}^2} + \frac{\cos^2 \theta \sin^2 \theta}{C_{66}} \right) \quad (3)$$

$$\epsilon'(\theta) = \begin{bmatrix} \cos \theta & -\sin \theta \\ \sin \theta & \cos \theta \end{bmatrix} \begin{bmatrix} 1 + \epsilon(\theta) & 0 \\ 0 & 1 - \epsilon(\theta)\nu(\theta) \end{bmatrix} \begin{bmatrix} \cos \theta & \sin \theta \\ -\sin \theta & \cos \theta \end{bmatrix} \quad (4)$$

$$R' = R\epsilon'(\theta) \quad (5)$$

where,  $\sigma$  denotes the magnitude of the externally applied stress.<sup>8</sup> The R is original lattice, while R' denotes the lattice with strain along the  $\theta$  direction.

To investigate the dynamics of photogenerated carriers in the  $M_2C_4X_4$ , the ab initio NAMD simulations are conducted using Hefei-NAMD code,<sup>9</sup> which augments the VASP with the NAMD capabilities within time-dependent density functional theory (TDDFT). After geometry optimization, we use the velocity rescaling to bring the temperature of the system to 300 K. Then, a 6.0 ps microcanonical ab initio molecular dynamics (MD) trajectory is then generated using a 1.0 fs time step. The NAMD results are based on an average over 100 different initial configurations obtained from the MD trajectory. For each chosen structure, we sample  $2 \times 10^4$  trajectories for the last 2.0 ps.

In order to study the optical properties of  $M_2C_4X_4$ , the light absorption coefficient is evaluated by the following equation:<sup>10</sup>

$$\alpha(\omega) = \frac{\sqrt{2}\omega}{c} \left[ \sqrt{\varepsilon_1^2(\omega) + \varepsilon_2^2(\omega)} - \varepsilon_1(\omega) \right]^{1/2} \quad (6)$$

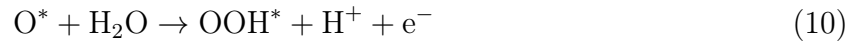
where  $\omega$  and  $c$  denote the frequency of incident light and light velocity, respectively.  $\varepsilon_1$  and  $\varepsilon_2$  represent the real and imaginary parts of the dielectric function, which can be calculated by the usual Kramers-Kronig transformation and summation over empty states, respectively.<sup>11</sup>

The Gibbs free energies for the photocatalytic redox reaction of water were evaluated at 298 K and 1 atm according to the formula:<sup>12</sup>

$$G = H - T\Delta S = E_{\text{DFT}} + E_{\text{ZPE}} + \int_0^{298K} C_v dT - T\Delta S \quad (7)$$

where  $E_{\text{DFT}}$  and  $E_{\text{ZPE}}$  are the total energy and the zero-point vibrational energy obtained from the DFT calculation,  $\int_0^{298K} C_v dT$  is the heat capacity, representing the total energy change when the system is heated from 0 K to 298 K.  $T$  and  $\Delta S$  are the temperature and the entropy.

The oxygen evolution reaction (OER) transforming water ( $\text{H}_2\text{O}$ ) into oxygen ( $\text{O}_2$ ) is decomposed into four electron steps:



The process of the hydrogen evolution reaction (HER) can be written by the following steps:



In our calculations, the light-induced driven potential for the HER is evaluated as the energy difference between the hydrogen reduction potential and the CBM, while the potential of photogenerated holes for water oxidation is calculated as the energy difference between the hydrogen reduction potential and the VBM.

Thus, the Gibbs free energy differences under different pH and extra potential bias can be calculated:

$$\Delta G(4) = G_{\text{OH}^*} + 1/2G_{\text{H}_2} - G_* - G_{\text{H}_2\text{O}} + G_{\text{U}} - G_{\text{pH}} \quad (14)$$

$$\Delta G(5) = G_{\text{O}^*} + 1/2G_{\text{H}_2} - G_{\text{OH}^*} + G_{\text{U}} - G_{\text{pH}} \quad (15)$$

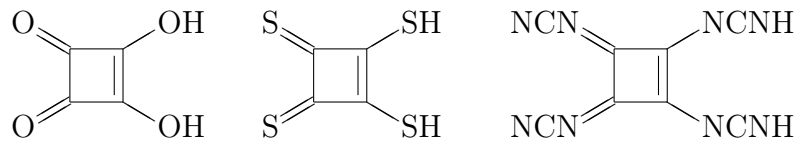
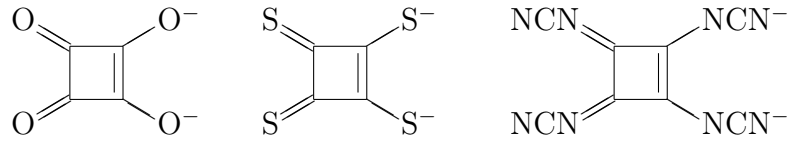
$$\Delta G(6) = G_{\text{OOH}^*} + 1/2G_{\text{H}_2} - G_{\text{O}^*} - G_{\text{H}_2\text{O}} + G_{\text{U}} - G_{\text{pH}} \quad (16)$$

$$\Delta G(7) = G_{\text{O}_2} + 1/2G_{\text{H}_2} + G_* - G_{\text{OOH}^*} + G_{\text{U}} - G_{\text{pH}} \quad (17)$$

$$\Delta G(8) = G_{\text{H}^*} - 1/2G_{\text{H}_2} - G_* + G_{\text{U}} + G_{\text{pH}} \quad (18)$$

$$\Delta G(9) = G_{\text{H}_2} + G_* - G_{\text{H}^*} - 1/2G_{\text{H}_2} + G_{\text{U}} + G_{\text{pH}} \quad (19)$$

The chemical structures of three cyclobutadiene derivatives ( $C_4O_4^{2-}$ ,  $C_4S_4^{2-}$ , and  $C_4(NCN)_4^{2-}$ ), along with their corresponding acids ( $H_2C_4O_4$ ,  $H_2C_4S_4$ , and  $H_2C_4(NCN)_4$ ), are provided below, along with the structural information for  $Cu_2O$ .



$Cu_4O_2$

1.00000000000000

4.3059209817536424 0.0000000000000000 0.0000000000000000

0.0000000000000000 4.3059209817536424 0.0000000000000000

0.0000000000000000 0.0000000000000000 4.3059209817536424

$Cu$  O

4 2

Direct

0.2500000000000000 0.2500000000000000 0.7500000000000000

0.7500000000000000 0.2500000000000000 0.2500000000000000

0.2500000000000000 0.7500000000000000 0.2500000000000000

0.7500000000000000 0.7500000000000000 0.7500000000000000

0.5000000000000000 0.5000000000000000 0.5000000000000000

0.0000000000000000 0.0000000000000000 0.0000000000000000

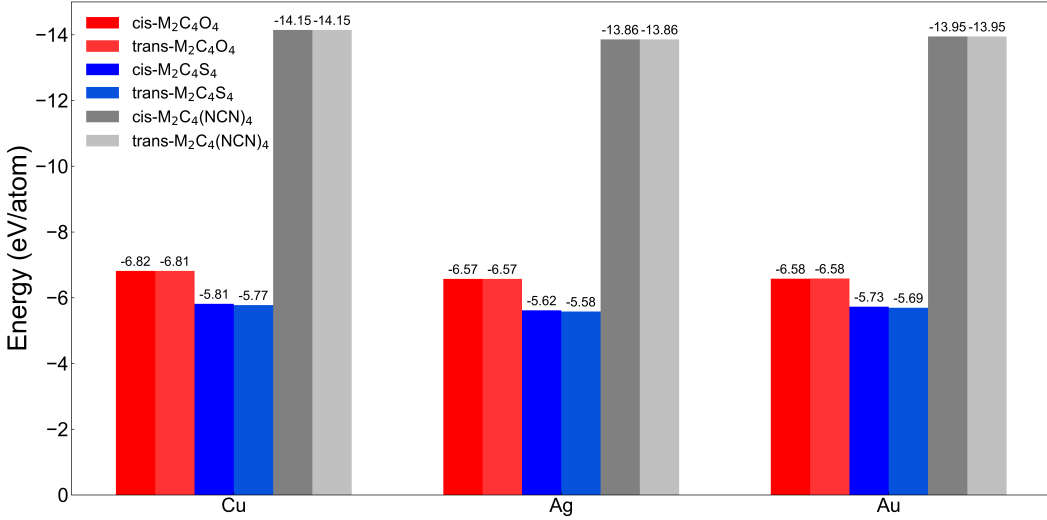


Figure S1: Average energy of  $M_2C_4X_4$ .

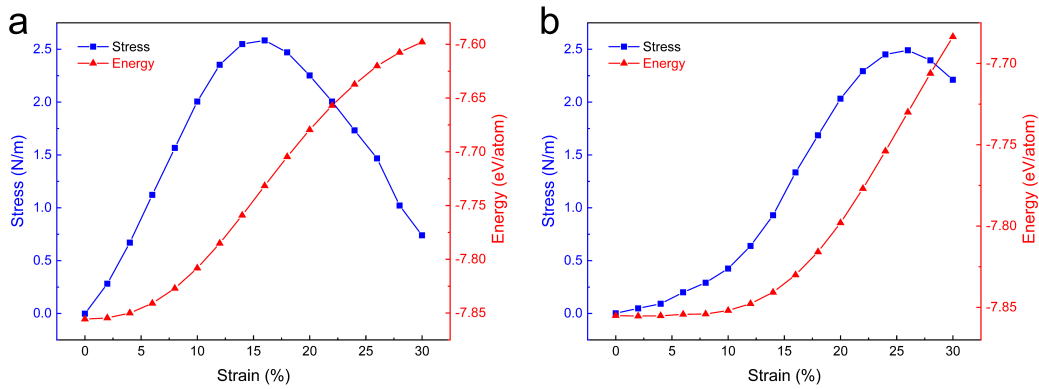


Figure S2: The blue illustrates the stress-strain relationship for (a) cis- (b) trans- $Cu_2C_4(NCN)_4$ , while red depicts the correlation between strain and average energy (eV/atom). It is worth noting that we use  $\sqrt{2} \times \sqrt{2}$  supercell for the trans- $Cu_2C_4(NCN)_4$  structure to keep the consistent of strain direction.

For HER, a proton  $H^+$  and an electron form a  $H^*$  at the N sites with a high  $\Delta G = 1.87$  eV without irradiation. The  $H^*$  then combines a proton and an electron to form hydrogen, releasing energy of 1.46 eV. Upon irradiation, an external potential ( $U_e = 0.83$  V) is introduced by the photogenerated electron, defined as the energy difference between the CBM and the hydrogen reduction potential. Then the  $\Delta G$  is reduced to 1.04 eV. In acidic environments, for pH = 1, the reaction barrier is further reduced to 0.69 eV.

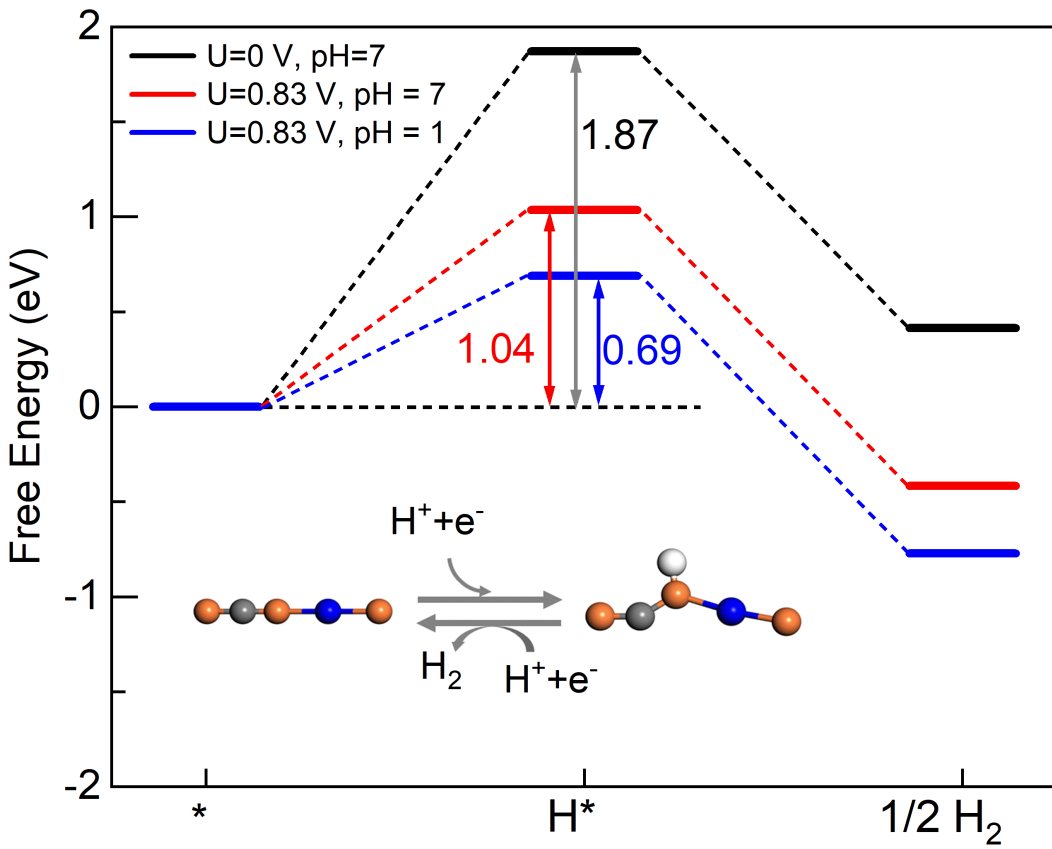


Figure S3: Free energy diagrams of HER on the  $\text{cis-Cu}_2\text{C}_4(\text{NCN})_4$  under different conditions. Proposed photocatalytic pathways of water hydrogen reduction half-reactions with the most energetically favorable absorbed intermediates ( $\text{H}^*$ ) on the  $\text{cis-Cu}_2\text{C}_4(\text{NCN})_4$ . The grey, blue, orange, and white balls represent C, Cu, N, and H atoms, respectively.

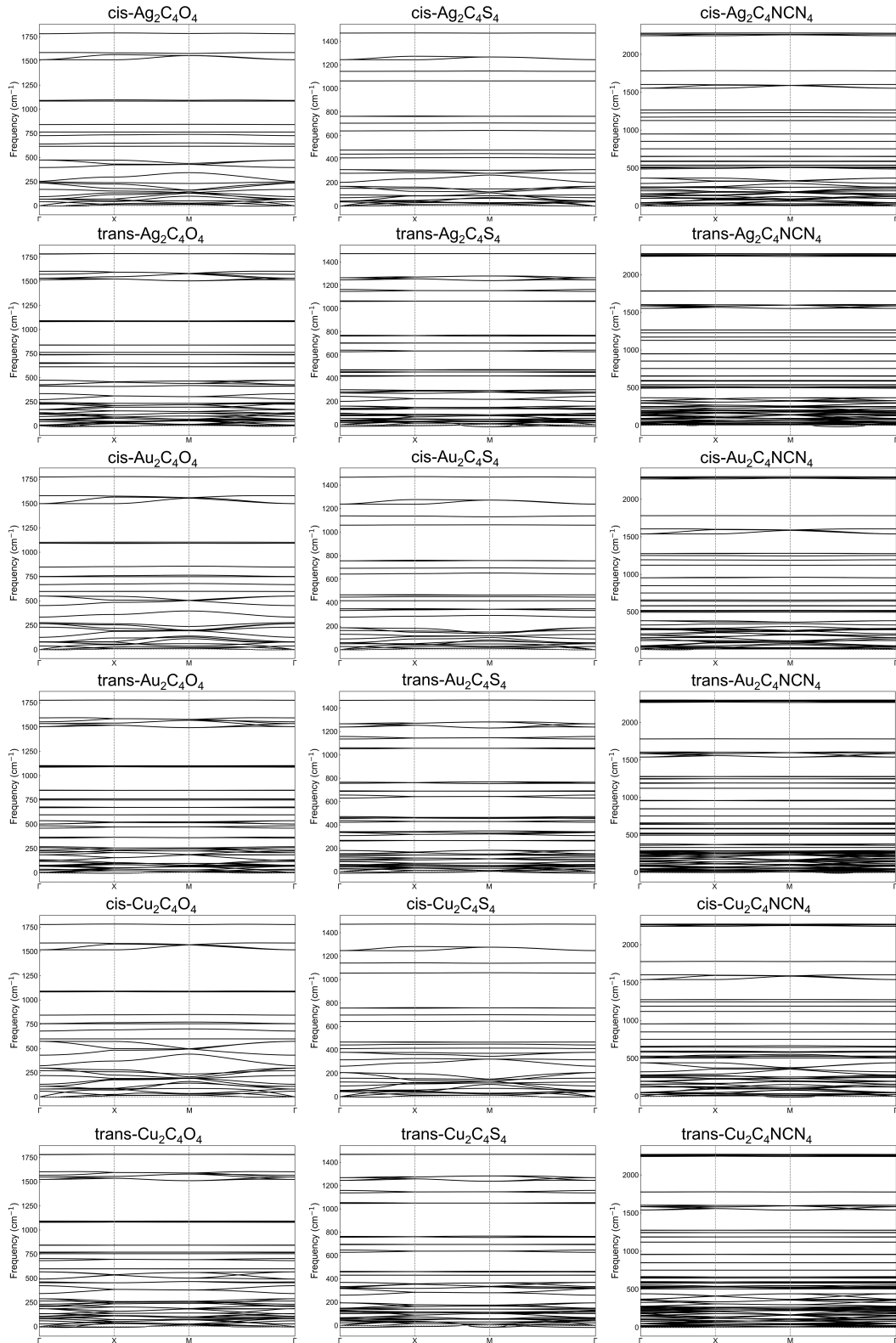


Figure S4: Phonon spectra of  $M_2C_4X_4$ .

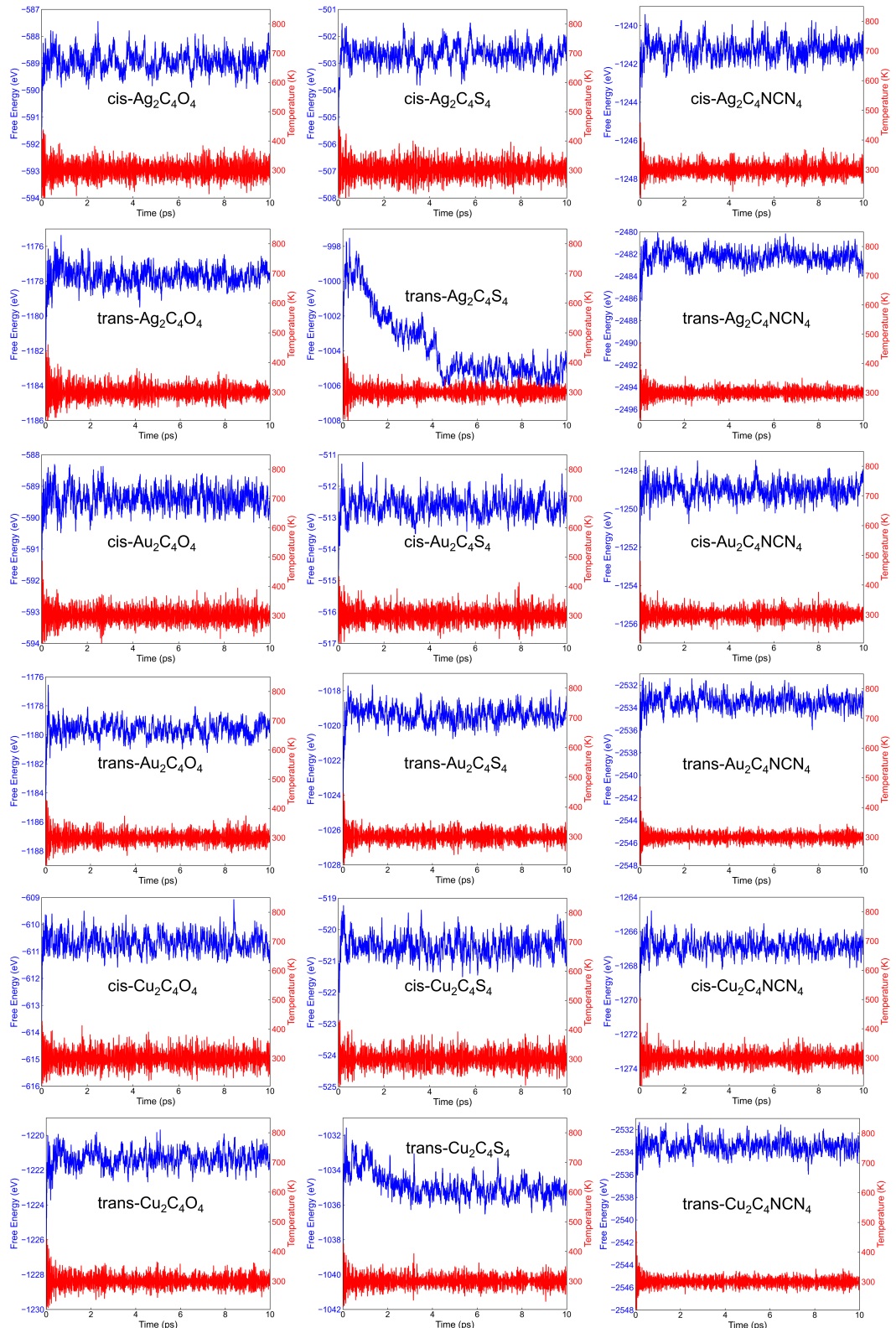


Figure S5: Free energy of  $M_2C_4X_4$  with respect to simulation time at 300 K.

# The structure information of $M_2C_4X_4$

cis-Ag-NCN

1.000000000000000

12.5081807006695662 -0.0000002655152185 0.00000000000000000000

0.00000026551521850 12.508180700669566 0.00000000000000000000

0.00000000000000000000 0.00000000000000000000 15.00000000000000000000

Ag C N

2 8 8

Direct

0.5000000000000000 0.0000000000000000 0.5000000000000000

0.0000000000000000 0.5000000000000000 0.5000000000000000

0.5424164917667159 0.4292284159163318 0.5000000000000000

0.4339204774846479 0.7542053660226586 0.5000000000000000

0.5707715840836681 0.5424164917667159 0.5000000000000000

0.2457946339773412 0.4339204774846479 0.5000000000000000

0.4575835082332840 0.5707715840836681 0.5000000000000000

0.5660795225153521 0.2457946339773412 0.5000000000000000

0.4292284159163318 0.4575835082332840 0.5000000000000000

0.7542053660226586 0.5660795225153521 0.5000000000000000

0.3978472943637277 0.6573280224490148 0.5000000000000000

0.4528224042970317 0.8464247672229176 0.5000000000000000

0.3426719775509852 0.3978472943637277 0.5000000000000000

0.1535752327770825 0.4528224042970317 0.5000000000000000

0.6021527056362723 0.3426719775509852 0.5000000000000000

0.5471775957029684 0.1535752327770825 0.5000000000000000

0.6573280224490148 0.6021527056362723 0.5000000000000000

0.8464247672229176 0.5471775957029684 0.5000000000000000

cis-Ag-O

1.00000000000000

7.7086358869345926 -0.0000000397228169 0.000000000000000000

0.0000000397228169 7.70863588693459260 0.000000000000000000

0.000000000000000000 0.000000000000000000 15.000000000000000000

Ag C O

2 4 4

Direct

0.000000000000000000 0.500000000000000000 0.500000000000000000

0.500000000000000000 0.000000000000000000 0.500000000000000000

0.5605457829761124 0.3795222337544306 0.500000000000000000

0.4394542170238878 0.6204777662455694 0.500000000000000000

0.6204777662455694 0.5605457829761124 0.500000000000000000

0.3795222337544306 0.4394542170238878 0.500000000000000000

0.7645202657744820 0.6390771638092003 0.500000000000000000

0.2354797342255181 0.3609228361907997 0.500000000000000000

0.3609228361907997 0.7645202657744820 0.500000000000000000

0.6390771638092003 0.2354797342255181 0.500000000000000000

cis-Ag-S

1.00000000000000

7.97351847260658350 0.0000000159476411 0.000000000000000000

-0.0000000159476411 7.9735184726065835 0.000000000000000000

0.000000000000000000 0.000000000000000000 15.000000000000000000

Ag C S

2 4 4

Direct

0.500000000000000 -0.000000000000000 0.500000000000000  
0.000000000000000 0.500000000000000 0.500000000000000  
0.5738517404731953 0.3936981571352673 0.500000000000000  
0.4261482595268046 0.6063018428647328 0.500000000000000  
0.6063018428647328 0.5738517404731953 0.500000000000000  
0.3936981571352673 0.4261482595268046 0.500000000000000  
0.7737886774848449 0.6977337900351044 0.500000000000000  
0.2262113225151550 0.3022662099648957 0.500000000000000  
0.3022662099648957 0.7737886774848449 0.500000000000000  
0.6977337900351044 0.2262113225151550 0.500000000000000

cis-Au-NCN

1.00000000000000  
12.4238869995591905 -0.000000859394267 0.000000000000000  
0.0000008593942670 12.4238869995591905 0.000000000000000  
0.000000000000000 0.000000000000000 15.000000000000000

Au C N

2 8 8

Direct

0.500000000000000 0.000000000000000 0.500000000000000  
0.000000000000000 0.500000000000000 0.500000000000000  
0.5412598646651132 0.4279279029157148 0.500000000000000  
0.4378397700002808 0.7572558385399885 0.500000000000000  
0.5720720970842851 0.5412598646651132 0.500000000000000  
0.2427441614600116 0.4378397700002808 0.500000000000000  
0.4587401353348867 0.5720720970842851 0.500000000000000

0.5621602299997192 0.2427441614600116 0.5000000000000000  
0.4279279029157148 0.4587401353348867 0.5000000000000000  
0.7572558385399885 0.5621602299997192 0.5000000000000000  
0.4003494381992337 0.6603993324242404 0.5000000000000000  
0.4574485032062731 0.8498665433543918 0.5000000000000000  
0.3396006675757597 0.4003494381992337 0.5000000000000000  
0.1501334566456083 0.4574485032062731 0.5000000000000000  
0.5996505618007664 0.3396006675757597 0.5000000000000000  
0.5425514967937268 0.1501334566456083 0.5000000000000000  
0.6603993324242404 0.5996505618007664 0.5000000000000000  
0.8498665433543918 0.5425514967937268 0.5000000000000000

#### cis-Au-O

1.00000000000000  
7.6349634338847805 -0.00000004497056450 0.0000000000000000  
0.0000000449705645 7.63496343388478050 0.0000000000000000  
0.0000000000000000 0.0000000000000000 15.0000000000000000

#### Au C O

2 4 4

#### Direct

0.5000000000000000 0.0000000000000000 0.5000000000000000  
0.0000000000000000 0.5000000000000000 0.5000000000000000  
0.5561200480781908 0.3763723788874117 0.5000000000000000  
0.4438799519218091 0.6236276511125908 0.5000000000000000  
0.6236276511125908 0.5561200480781908 0.5000000000000000  
0.3763723788874117 0.4438799519218091 0.5000000000000000  
0.7709388406483946 0.6327674061127904 0.5000000000000000

0.2290611593516055 0.3672325938872097 0.5000000000000000  
0.3672325938872097 0.7709388406483946 0.5000000000000000  
0.6327674061127904 0.2290611593516055 0.5000000000000000

cis-Au-S

1.000000000000000  
8.04542968039379150 0.0000062103418392 0.0000000000000000  
-0.0000062103418392 8.0454296803937915 0.0000000000000000  
0.0000000000000000 0.0000000000000000 15.000000000000000

Au C S

2 4 4

Direct

0.000000000000000 0.500000000000000 0.500000000000000  
0.500000000000000 0.000000000000000 0.500000000000000  
0.5668368643827414 0.3905987994227461 0.500000000000000  
0.4331631356172586 0.6094012005772540 0.500000000000000  
0.6094012005772540 0.5668368643827414 0.500000000000000  
0.3905987994227461 0.4331631356172586 0.500000000000000  
0.7807097661486294 0.6829618155534493 0.500000000000000  
0.2192902338513707 0.3170381844465508 0.500000000000000  
0.3170381844465508 0.7807097661486294 0.500000000000000  
0.6829618155534493 0.2192902338513707 0.500000000000000

cis-Cu-NCN

1.000000000000000  
12.1231191754076626 -0.00001671144597760 0.0000000000000000  
0.00001671144597760 12.1231191754076608 0.0000000000000000

0.0000000000000000 0.0000000000000000 15.000000000000000

Cu C N

2 8 8

Direct

0.5000000000000000 0.0000000000000000 0.5000000000000000

0.0000000000000000 0.5000000000000000 0.5000000000000000

0.5423306526405938 0.4261763214612344 0.5000000000000000

0.4366905083676969 0.7635566134460632 0.5000000000000000

0.5738236785387656 0.5423306526405938 0.5000000000000000

0.2364433865539297 0.4366905083676969 0.5000000000000000

0.4576693473594062 0.5738236785387656 0.5000000000000000

0.5633094916323031 0.2364433865539297 0.5000000000000000

0.4261763214612344 0.4576693473594062 0.5000000000000000

0.7635566134460632 0.5633094916323031 0.5000000000000000

0.3979347170905143 0.6644556047056227 0.5000000000000000

0.4576732762848081 0.8585591196620896 0.5000000000000000

0.3355443952943844 0.3979347170905143 0.5000000000000000

0.1414408803379104 0.4576732762848081 0.5000000000000000

0.6020652829094857 0.3355443952943844 0.5000000000000000

0.5423267237151919 0.1414408803379104 0.5000000000000000

0.6644556047056227 0.6020652829094857 0.5000000000000000

0.8585591196620896 0.5423267237151919 0.5000000000000000

cis-Cu-O

1.000000000000000

7.40796703809758750 0.0000000698134758 0.0000000000000000

-0.0000000698134758 7.4079670380975875 0.0000000000000000

0.0000000000000000 0.0000000000000000 15.000000000000000

Cu C O

2 4 4

Direct

-0.0000000000000000 0.5000000000000000 0.5000000000000000

0.5000000000000000 0.0000000000000000 0.5000000000000000

0.5529890894253555 0.3703844929715250 0.5000000000000000

0.4470109105746444 0.6296155070284750 0.5000000000000000

0.6296155070284750 0.5529890894253555 0.5000000000000000

0.3703844929715250 0.4470109105746444 0.5000000000000000

0.7852625282698603 0.6242376499246628 0.5000000000000000

0.2147374717301396 0.3757623500753371 0.5000000000000000

0.3757623500753371 0.7852625282698603 0.5000000000000000

0.6242376499246628 0.2147374717301396 0.5000000000000000

cis-Cu-S

1.000000000000000

7.695499897000004 0.0000000000000000 0.0000000000000000

0.0000000000000000 7.695499897000004 0.0000000000000000

0.0000000000000000 0.0000000000000000 15.000000000000000

Cu C S

2 4 4

Direct

0.5000000000000000 0.0000000000000000 0.5000000000000000

0.0000000000000000 0.5000000000000000 0.5000000000000000

0.5702900289999988 0.3860099910000017 0.5000000000000000

0.4297099710000012 0.6139900089999983 0.5000000000000000

0.6139900089999983 0.5702900289999988 0.5000000000000000  
0.3860099910000017 0.4297099710000012 0.5000000000000000  
0.7940700050000018 0.6902800200000030 0.5000000000000000  
0.2059299949999982 0.3097199799999970 0.5000000000000000  
0.3097199799999970 0.7940700050000018 0.5000000000000000  
0.6902800200000030 0.2059299949999982 0.5000000000000000

trans-Ag-NCN

1.000000000000000  
16.6089072976612648 0.0000000000000000 0.0000000000000000  
0.0000000000000000 16.6089072976612648 0.0000000000000000  
0.0000000000000000 0.0000000000000000 15.000000000000000

Ag C N

4 16 16

Direct

0.3378093211950670 0.8378093211950670 0.5000000000000000  
0.1621906788049330 0.3378093211950670 0.5000000000000000  
0.6621906788049330 0.1621906788049330 0.5000000000000000  
0.8378093211950670 0.6621906788049330 0.5000000000000000  
0.0617773480998594 0.0066782605208644 0.5000000000000000  
0.8054119379843812 0.0351454626342118 0.5000000000000000  
0.9933217394791356 0.0617773480998594 0.5000000000000000  
0.9648545373657882 0.8054119379843812 0.5000000000000000  
0.9382226519001335 0.9933217394791356 0.5000000000000000  
0.1945880620156188 0.9648545373657882 0.5000000000000000  
0.0066782605208644 0.9382226519001335 0.5000000000000000  
0.0351454626342118 0.1945880620156188 0.5000000000000000

0.4382226519001335 0.5066782605208644 0.5000000000000000  
0.6945880620156188 0.5351454626342118 0.5000000000000000  
0.5066782605208644 0.5617773480998665 0.5000000000000000  
0.5351454626342118 0.3054119379843812 0.5000000000000000  
0.5617773480998665 0.4933217394791356 0.5000000000000000  
0.3054119379843812 0.4648545373657882 0.5000000000000000  
0.4933217394791356 0.4382226519001335 0.5000000000000000  
0.4648545373657882 0.6945880620156188 0.5000000000000000  
0.8601713923275653 0.9798054014717792 0.5000000000000000  
0.7483352603991449 0.0772090492675375 0.5000000000000000  
0.0201945985282208 0.8601713923275653 0.5000000000000000  
0.9227909507324625 0.7483352603991449 0.5000000000000000  
0.1398286076724347 0.0201945985282208 0.5000000000000000  
0.2516647396008551 0.9227909507324625 0.5000000000000000  
0.9798054014717792 0.1398286076724347 0.5000000000000000  
0.0772090492675375 0.2516647396008551 0.5000000000000000  
0.6398286076724347 0.4798054014717792 0.5000000000000000  
0.7516647396008551 0.5772090492675375 0.5000000000000000  
0.4798054014717792 0.3601713923275653 0.5000000000000000  
0.5772090492675375 0.2483352603991449 0.5000000000000000  
0.3601713923275653 0.5201945985282208 0.5000000000000000  
0.2483352603991449 0.4227909507324625 0.5000000000000000  
0.5201945985282208 0.6398286076724347 0.5000000000000000  
0.4227909507324625 0.7516647396008551 0.5000000000000000

trans-Ag-O

1.000000000000000

9.7743937177677971 0.0000000000000000 0.0000000000000000  
0.0000000000000000 9.7743937177677971 0.0000000000000000  
0.0000000000000000 0.0000000000000000 15.0000000000000000

Ag C O

4 8 8

Direct

0.3805465488961914 0.8805465488961914 0.5000000000000000  
0.1194534511038086 0.3805465488961914 0.5000000000000000  
0.6194534511038086 0.1194534511038086 0.5000000000000000  
0.8805465488961914 0.6194534511038086 0.5000000000000000  
0.1054417590822823 0.0141275003797929 0.5000000000000000  
0.9858724996202071 0.1054417590822823 0.5000000000000000  
0.8945582409177177 0.9858724996202071 0.5000000000000000  
0.0141275003797929 0.8945582409177177 0.5000000000000000  
0.3945582409177177 0.5141275003797929 0.5000000000000000  
0.5141275003797929 0.6054417590822823 0.5000000000000000  
0.6054417590822823 0.4858724996202071 0.5000000000000000  
0.4858724996202071 0.3945582409177177 0.5000000000000000  
0.7672201898749051 0.9634683429052870 0.5000000000000000  
0.0365316570947130 0.7672201898749051 0.5000000000000000  
0.2327798101250949 0.0365316570947130 0.5000000000000000  
0.9634683429052870 0.2327798101250949 0.5000000000000000  
0.7327798101250949 0.4634683429052870 0.5000000000000000  
0.4634683429052870 0.2672201898749051 0.5000000000000000  
0.2672201898749051 0.5365316570947130 0.5000000000000000  
0.5365316570947130 0.7327798101250949 0.5000000000000000

trans-Ag-S

1.000000000000000

11.1451644145435136 0.000000000000000000 0.000000000000000000

0.000000000000000000 11.1451644145435136 0.000000000000000000

0.000000000000000000 0.000000000000000000 15.0000000000000000

Ag C S

4 8 8

Direct

0.3439961595906494 0.8439961595906497 0.500000000000000000

0.1560038404093506 0.3439961595906494 0.500000000000000000

0.6560038404093503 0.1560038404093506 0.500000000000000000

0.8439961595906497 0.6560038404093503 0.500000000000000000

0.0921429448236903 0.0089849241428836 0.500000000000000000

0.9910150758571165 0.0921429448236903 0.500000000000000000

0.9078570551763098 0.9910150758571165 0.500000000000000000

0.0089849241428836 0.9078570551763098 0.500000000000000000

0.4078570551763095 0.5089849241428835 0.500000000000000000

0.5089849241428835 0.5921429448236902 0.500000000000000000

0.5921429448236902 0.4910150758571165 0.500000000000000000

0.4910150758571165 0.4078570551763095 0.500000000000000000

0.7608157845982013 0.9687183604749554 0.500000000000000000

0.0312816395250447 0.7608157845982013 0.500000000000000000

0.2391842154017986 0.0312816395250447 0.500000000000000000

0.9687183604749554 0.2391842154017986 0.500000000000000000

0.7391842154017987 0.4687183604749551 0.500000000000000000

0.4687183604749551 0.2608157845982014 0.500000000000000000

0.2608157845982014 0.5312816395250446 0.500000000000000000

0.5312816395250446 0.7391842154017987 0.5000000000000000

trans-Au-NCN

1.000000000000000

16.6151950007176197 0.0000000000000000 0.0000000000000000

0.0000000000000000 16.6151950007176232 0.0000000000000000

0.0000000000000000 0.0000000000000000 15.0000000000000000

Au C N

4 16 16

Direct

0.6677197642127268 0.1677197642127269 0.5000000000000000

0.3322802357872731 0.8322802357872732 0.5000000000000000

0.1677197642127269 0.3322802357872731 0.5000000000000000

0.8322802357872732 0.6677197642127268 0.5000000000000000

0.4958005990805847 0.4380406219066907 0.5000000000000000

0.5041994009194154 0.5619593780933021 0.5000000000000000

0.4380406219066907 0.5041994009194154 0.5000000000000000

0.5619593780933021 0.4958005990805847 0.5000000000000000

0.9958005990805846 0.0619593780933093 0.5000000000000000

0.0041994009194153 0.9380406219066979 0.5000000000000000

0.9380406219066979 0.9958005990805846 0.5000000000000000

0.0619593780933093 0.0041994009194153 0.5000000000000000

0.4576054761387802 0.6932291633480828 0.5000000000000000

0.5423945238612197 0.3067708366519173 0.5000000000000000

0.6932291633480828 0.5423945238612197 0.5000000000000000

0.3067708366519173 0.4576054761387802 0.5000000000000000

0.9576054761387803 0.8067708366519172 0.5000000000000000

0.0423945238612197 0.1932291633480827 0.5000000000000000  
 0.1932291633480827 0.9576054761387803 0.5000000000000000  
 0.8067708366519172 0.0423945238612197 0.5000000000000000  
 0.5145800045457326 0.6404631261369325 0.5000000000000000  
 0.4854199954542674 0.3595368738630745 0.5000000000000000  
 0.6404631261369325 0.4854199954542674 0.5000000000000000  
 0.3595368738630745 0.5145800045457326 0.5000000000000000  
 0.0145800045457326 0.8595368738630675 0.5000000000000000  
 0.9854199954542674 0.1404631261369253 0.5000000000000000  
 0.1404631261369253 0.0145800045457326 0.5000000000000000  
 0.8595368738630675 0.9854199954542674 0.5000000000000000  
 0.4141922481624045 0.7491511017883736 0.5000000000000000  
 0.5858077518375957 0.2508488982116265 0.5000000000000000  
 0.7491511017883736 0.5858077518375957 0.5000000000000000  
 0.2508488982116265 0.4141922481624045 0.5000000000000000  
 0.9141922481624043 0.7508488982116264 0.5000000000000000  
 0.0858077518376027 0.2491511017883807 0.5000000000000000  
 0.2491511017883807 0.9141922481624043 0.5000000000000000  
 0.7508488982116264 0.0858077518376027 0.5000000000000000

### trans-Au-O

1.00000000000000  
 9.6347693568091959 0.0000000000000000 0.0000000000000000  
 0.0000000000000000 9.6347693568091977 0.0000000000000000  
 0.0000000000000000 0.0000000000000000 15.0000000000000000

### Au C O

4 8 8

Direct

0.6191520646053413 0.1191520646053413 0.5000000000000000  
0.3808479353946587 0.8808479353946587 0.5000000000000000  
0.8808479353946587 0.6191520646053413 0.5000000000000000  
0.1191520646053413 0.3808479353946587 0.5000000000000000  
0.4880401655141978 0.3930440602251433 0.5000000000000000  
0.5119598344858022 0.6069559397748567 0.5000000000000000  
0.6069559397748567 0.4880401655141978 0.5000000000000000  
0.3930440602251433 0.5119598344858022 0.5000000000000000  
0.0119598344858022 0.8930440602251433 0.5000000000000000  
0.9880401655141978 0.1069559397748567 0.5000000000000000  
0.8930440602251433 0.9880401655141978 0.5000000000000000  
0.1069559397748567 0.0119598344858022 0.5000000000000000  
0.5340484743408787 0.7365653085455584 0.5000000000000000  
0.4659515256591213 0.2634346914544416 0.5000000000000000  
0.2634346914544416 0.5340484743408787 0.5000000000000000  
0.7365653085455584 0.4659515256591213 0.5000000000000000  
0.9659515256591213 0.2365653085455584 0.5000000000000000  
0.0340484743408786 0.7634346914544416 0.5000000000000000  
0.2365653085455584 0.0340484743408786 0.5000000000000000  
0.7634346914544416 0.9659515256591213 0.5000000000000000

trans-Au-S

1.000000000000000  
11.0108003615999994 0.0000000000000000 0.0000000000000000  
0.0000000000000000 11.0108003615999994 0.0000000000000000  
0.0000000000000000 0.0000000000000000 15.000000000000000

Au C S

4 8 8

Direct

0.3597500030000020 0.8597499729999996 0.5000000000000000  
0.6402499679999991 0.1402500270000004 0.5000000000000000  
0.1402500270000004 0.3597500030000020 0.5000000000000000  
0.8597499729999996 0.6402499679999991 0.5000000000000000  
0.0933699980000000 0.0074699999999979 0.5000000000000000  
0.9066299799999982 0.9925299880000011 0.5000000000000000  
0.9925299880000011 0.0933699980000000 0.5000000000000000  
0.007469999999979 0.9066299799999982 0.5000000000000000  
0.4066300089999970 0.5074700119999989 0.5000000000000000  
0.5933700200000018 0.4925299880000011 0.5000000000000000  
0.5074700119999989 0.5933700200000018 0.5000000000000000  
0.4925299880000011 0.4066300089999970 0.5000000000000000  
0.7577599879999966 0.9682300090000027 0.5000000000000000  
0.2422400120000034 0.0317699909999973 0.5000000000000000  
0.0317699909999973 0.7577599879999966 0.5000000000000000  
0.9682300090000027 0.2422400120000034 0.5000000000000000  
0.7422400120000034 0.4682300090000027 0.5000000000000000  
0.2577599879999966 0.5317699909999973 0.5000000000000000  
0.4682300090000027 0.2577599879999966 0.5000000000000000  
0.5317699909999973 0.7422400120000034 0.5000000000000000

trans-Cu-NCN

1.000000000000000

16.0620465284148430 0.0000000000000000 0.0000000000000000

0.0000000000000000 16.0620465284148430 0.0000000000000000

0.0000000000000000 0.0000000000000000 15.0000000000000000

Cu C N

4 16 16

Direct

0.3394703236030632 0.8394703536030586 0.5000000000000000

0.6605296463969414 0.1605296463969414 0.5000000000000000

0.1605296463969414 0.3394703236030632 0.5000000000000000

0.8394703536030586 0.6605296463969414 0.5000000000000000

0.0639607283263995 0.0060408653487577 0.5000000000000000

0.9360392566735957 0.9939591576512407 0.5000000000000000

0.9939591576512407 0.0639607283263995 0.5000000000000000

0.0060408653487577 0.9360392566735957 0.5000000000000000

0.4360392566735958 0.5060408423487593 0.5000000000000000

0.5639607433264043 0.4939591276512382 0.5000000000000000

0.5060408423487593 0.5639607433264043 0.5000000000000000

0.4939591276512382 0.4360392566735958 0.5000000000000000

0.7990969013329081 0.0387018691023744 0.5000000000000000

0.2009030986670919 0.9612981448976269 0.5000000000000000

0.9612981448976269 0.7990969013329081 0.5000000000000000

0.0387018691023744 0.2009030986670919 0.5000000000000000

0.7009030986670919 0.5387018551023731 0.5000000000000000

0.2990969013329081 0.4612981448976268 0.5000000000000000

0.5387018551023731 0.2990969013329081 0.5000000000000000

0.4612981448976268 0.7009030986670919 0.5000000000000000

0.8551019164157045 0.9811490803541020 0.5000000000000000

0.1448980835842955 0.0188509196458980 0.5000000000000000

0.0188509196458980 0.8551019164157045 0.5000000000000000  
0.9811490803541020 0.1448980835842955 0.5000000000000000  
0.6448980835842955 0.4811490803541020 0.5000000000000000  
0.3551019164157045 0.5188509196458980 0.5000000000000000  
0.4811490803541020 0.3551019164157045 0.5000000000000000  
0.5188509196458980 0.6448980835842955 0.5000000000000000  
0.7403914434158366 0.0828282292805499 0.5000000000000000  
0.2596085565841634 0.9171717557194453 0.5000000000000000  
0.9171717557194453 0.7403914434158366 0.5000000000000000  
0.0828282292805499 0.2596085565841634 0.5000000000000000  
0.7596085565841634 0.5828282442805547 0.5000000000000000  
0.2403914434158366 0.4171717557194453 0.5000000000000000  
0.5828282442805547 0.2403914434158366 0.5000000000000000  
0.4171717557194453 0.7596085565841634 0.5000000000000000

#### trans-Cu-O

1.000000000000000  
9.4475414659485288 0.000000000000000 0.000000000000000  
0.000000000000000 9.4475414659485306 0.000000000000000  
0.000000000000000 0.000000000000000 15.000000000000000

#### Cu C O

4 8 8

#### Direct

0.3754365506924984 0.8754365506924984 0.5000000000000000  
0.1245634493075016 0.3754365506924984 0.5000000000000000  
0.6245634493075016 0.1245634493075016 0.5000000000000000  
0.8754365506924984 0.6245634493075016 0.5000000000000000

0.1097196690872053 0.0054240913012151 0.5000000000000000  
0.9945759086987849 0.1097196690872053 0.5000000000000000  
0.8902803309127876 0.9945759086987849 0.5000000000000000  
0.0054240913012151 0.8902803309127876 0.5000000000000000  
0.3902803309127947 0.5054240913012151 0.5000000000000000  
0.5054240913012151 0.6097196690872124 0.5000000000000000  
0.6097196690872124 0.4945759086987849 0.5000000000000000  
0.4945759086987849 0.3902803309127947 0.5000000000000000  
0.7567710105881673 0.9819440011803451 0.5000000000000000  
0.0180559988196549 0.7567710105881673 0.5000000000000000  
0.2432289894118327 0.0180559988196549 0.5000000000000000  
0.9819440011803451 0.2432289894118327 0.5000000000000000  
0.7432289894118327 0.4819440011803451 0.5000000000000000  
0.4819440011803451 0.2567710105881673 0.5000000000000000  
0.2567710105881673 0.5180559988196549 0.5000000000000000  
0.5180559988196549 0.7432289894118327 0.5000000000000000

### trans-Cu-S

1.000000000000000  
10.8598501692309934 0.0000000000000000 0.0000000000000000  
0.0000000000000000 10.8598501692309934 0.0000000000000000  
0.0000000000000000 0.0000000000000000 15.0000000000000000

### Cu C S

4 8 8

### Direct

0.3444541283288983 0.8444541283288982 0.5000000000000000  
0.1555458716711015 0.3444541283288983 0.5000000000000000

0.6555458716711018 0.1555458716711015 0.5000000000000000  
0.8444541283288982 0.6555458716711018 0.5000000000000000  
0.0949137910350539 0.0027638810577562 0.5000000000000000  
0.9972361189422437 0.0949137910350539 0.5000000000000000  
0.9050862089649385 0.9972361189422437 0.5000000000000000  
0.0027638810577562 0.9050862089649385 0.5000000000000000  
0.4050862089649462 0.5027638810577563 0.5000000000000000  
0.5027638810577563 0.5949137910350615 0.5000000000000000  
0.5949137910350615 0.4972361189422435 0.5000000000000000  
0.4972361189422435 0.4050862089649462 0.5000000000000000  
0.7527336544369295 0.9829141398586501 0.5000000000000000  
0.0170858601413497 0.7527336544369295 0.5000000000000000  
0.2472663455630704 0.0170858601413497 0.5000000000000000  
0.9829141398586501 0.2472663455630704 0.5000000000000000  
0.7472663455630705 0.4829141398586504 0.5000000000000000  
0.4829141398586504 0.2527336544369294 0.5000000000000000  
0.2527336544369294 0.5170858601413499 0.5000000000000000  
0.5170858601413499 0.7472663455630705 0.5000000000000000

## References

- (1) Kresse, G.; Furthmüller, J. Efficient iterative schemes for ab initio total-energy calculations using a plane-wave basis set. *Phys. Rev. B* **1996**, *54*, 11169.
- (2) Perdew, J. P.; Burke, K.; Ernzerhof, M. Generalized gradient approximation made simple. *Phys. Rev. Lett.* **1996**, *77*, 3865.
- (3) Blöchl, P. E. Projector augmented-wave method. *Phys. Rev. B* **1994**, *50*, 17953.
- (4) Monkhorst, H. J.; Pack, J. D. Special points for Brillouin-zone integrations. *Phys. Rev. B* **1976**, *13*, 5188.
- (5) Heyd, J.; Scuseria, G. E.; Ernzerhof, M. Hybrid functionals based on a screened Coulomb potential. *J. Chem. Phys.* **2003**, *118*, 8207–8215.
- (6) Paier, J.; Marsman, M.; Hummer, K.; Kresse, G.; Gerber, I. C.; Ángyán, J. G. Screened hybrid density functionals applied to solids. *J. Chem. Phys.* **2006**, *124*, 154709.
- (7) Wang, H.; Li, T.; Liu, X.; Zhu, W.; Chen, Z.; Li, Z.; Yang, J. mech2d: An Efficient Tool for High-Throughput Calculation of Mechanical Properties for Two-Dimensional Materials. *Molecules* **2023**, *28*, 4337.
- (8) Wang, L.; Kutana, A.; Zou, X.; Yakobson, B. I. Electro-mechanical anisotropy of phosphorene. *Nanoscale* **2015**, *7*, 9746–9751.
- (9) Zheng, Q.; Chu, W.; Zhao, C.; Zhang, L.; Guo, H.; Wang, Y.; Jiang, X.; Zhao, J. Ab initio nonadiabatic molecular dynamics investigations on the excited carriers in condensed matter systems. *Wiley Interdiscip. Rev. Comput. Mol. Sci.* **2019**, *9*, e1411.
- (10) Li, X.; Zhao, J.; Yang, J. Semihydrogenated BN sheet: a promising visible-light driven photocatalyst for water splitting. *Sci. Rep.* **2013**, *3*, 1858.

- (11) Gajdoš, M.; Hummer, K.; Kresse, G.; Furthmüller, J.; Bechstedt, F. Linear optical properties in the projector-augmented wave methodology. *Phys. Rev. B* **2006**, *73*, 045112.
- (12) Li, X.; Gong, H.; Zhuang, Q.; Wang, B.; Zheng, X.; Yang, J. Reaction on a Rink: Kondo-Enhanced Heterogeneous Single-Atom Catalysis. *J. Phys. Chem. C* **2021**, *125*, 21488–21495.